ORNL/TM-5731

Improved Gas Distributor for Coating HTGR Fuel Particles

W. J. Lackey
D. P. Stinton
J. D. Sease

OAK RIDGE NATIONAL LABORATORY
OPERATED BY UNION CARBIDE CORPORATION FOR THE ENERGY RESEARCH AND DEVELOPMENT ADMINISTRATION

DISCLAIMER

Printed in the United States of America. Available from
National Technical Information Service
U.S. Department of Commerce
5285 Port Royal Road, Springfield, Virginia 22161
Price: Printed Copy $4.00; Microfiche $3.00

ORNL/TM-5731
Distribution
Category UC-77

Contract No. W-7405-eng-26

METALS AND CERAMICS DIVISION

THORIUM UTILIZATION PROGRAM (189a OH045)

Refabrication Development - Task 300

IMPROVED GAS DISTRIBUTOR FOR COATING HTGR FUEL PARTICLES

W. J. Lackey, D. P. Stinton, and J. D. Sease

Date Published: January 1977

OAK RIDGE NATIONAL LABORATORY
Oak Ridge, Tennessee 37830
operated by
UNION CARBIDE CORPORATION
for the
ENERGY RESEARCH AND DEVELOPMENT ADMINISTRATION

THIS PAGE

WAS INTENTIONALLY

LEFT BLANK

CONTENTS

IMPROVED GAS DISTRIBUTOR FOR COATING HTGR FUEL PARTICLES

W. J. Lackey, D. P. Stinton, and J. D. Sease

ABSTRACT

A new and improved gas distributor was developed for use in coating fuel particles for the HTGR. The coating gas enters the coating furnace through multiple thin regions of a porous plate. This more uniformly disperses the gas and leads to improved coating properties. High-quality carbon and SiC coatings have been deposited with the new distributor in both 13- and 24-cm-diam coating furnaces.

INTRODUCTION

Coatings for thorium- and uranium-bearing fuel particles for High-Temperature Gas-Cooled Reactors consist of chemically vapor deposited carbon and silicon carbide. The coatings provide mechanical strength and retain fission products. Two types of pyrocarbon coatings are used: a low-density buffer and a higher density low-temperature isotropic (LTI) coating. By varying the type of hydrocarbon gas, deposition temperature, flow rate, etc., carbon coatings can be deposited with the desired properties. Silicon carbide coatings are deposited by the decomposition of CH_3Cl_3Si in the presence of hydrogen. All the coatings are deposited in a fluidized-bed coating furnace. [1,2]

The most important component of the coating furnace is the gas distributor, which brings the coating gases into contact with the fuel particles. The important criteria to be considered in design of the gas distributor are:

1. The distributor should ideally disperse the gas over the full area of the coating chamber to increase the particle-gas contact area.

This increases the uniformity of particle motion and the region within which coatings are deposited; it likewise reduces bubble size and violent particle surging.

2. The gas should not be excessively heated during its passage through the distributor. Otherwise it will partially decompose prematurely, causing excessive deposition within or on the distributor.

3. The distributor should be suitably designed and have sufficient mechanical integrity to virtually eliminate loss of particles from the coating chamber.

4. The distributor should provide for rapid and reliable discharge of hot particles from the furnace.

5. The distributor should be simple, inexpensive, reliable, and easily maintainable.

6. The distributor should be capable of depositing both carbon and SiC coatings of high quality as regards density, preferred orientation, permeability, fraction defective, and numerous other coating properties.

The most widely used type of gas distributor is a single-inlet cone or some variation, such as a two-fluid dual concentric inlet cone. Conical gas distributors as seen in Fig. 1(a) have been under development for about 15 years. The cone satisfies the previously mentioned criteria with three exceptions. The first is nonuniform distribution of coating gas over the bed of particles which along with the conical geometry of the coating chamber causes agglomeration of gas bubbles, a slugging bed action, and excessive throwing of particles. Second, particles can escape from the coating chamber through the gas inlet at the apex of the cone. If a malfunction or human error causes the gas flow to be significantly reduced during coating, heating, or cooling, particles will drain from the furnace. A third problem arises because particles do not always drain properly and as a result back up inside the cone. If this goes unnoticed, pyrophoric material may be exposed to air or remaining particles could contaminate the next coating run. The work area can also become contaminated if particles drain or spill from the cone during maintenance or replacement.

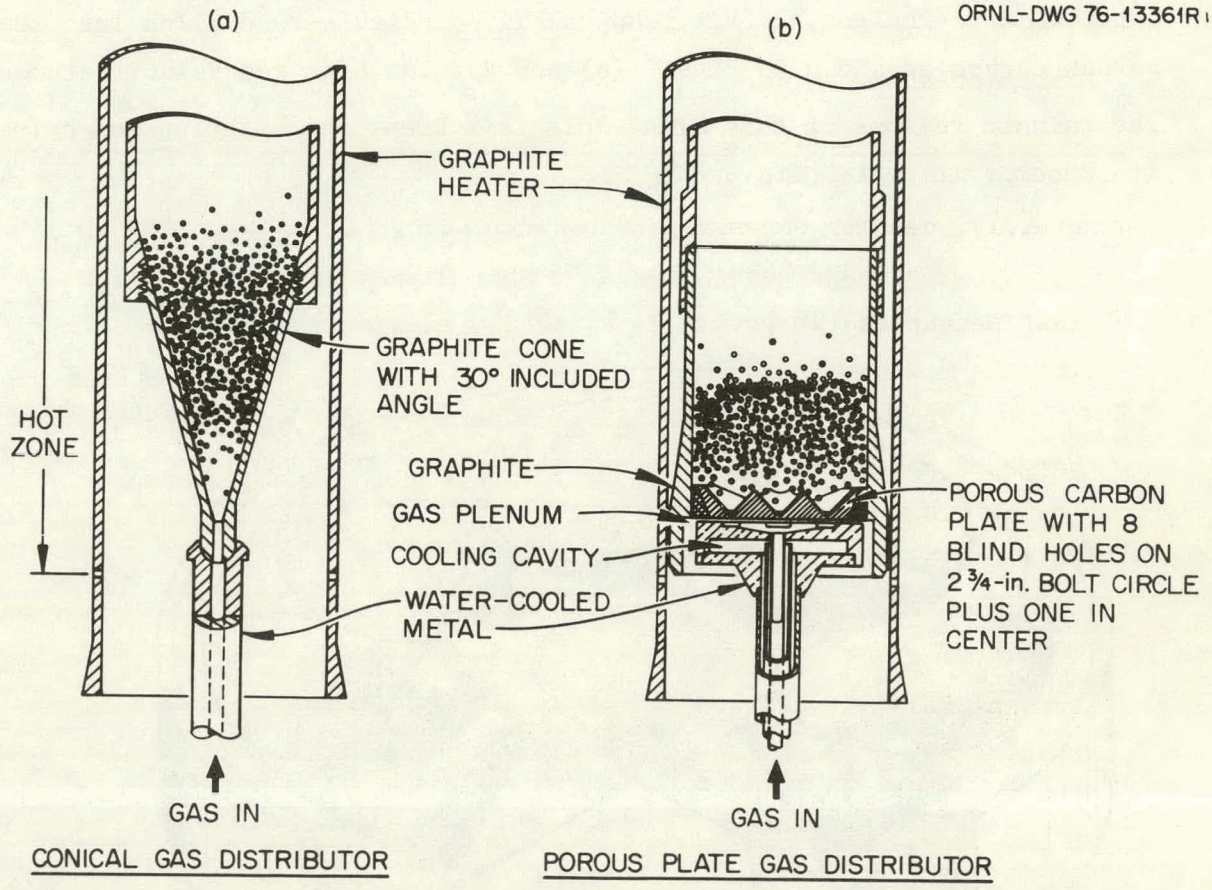

Fig. 1. Gas Distributors. (a) Conical. (b) Blind-hole porous plate.

Earlier gas distributors used multiple inlets protruding through either a porous carbon base or through an array of dense carbon cones,[3] but both approaches suffer from complexity, loss of particles through the multiple inlets, or variation in gas flow from inlet to inlet. Another design uses a uniform thickness of porous carbon as the gas distributor. This works well during the initial portion of the run but soon plugs, beginning at the perimeter, because of insufficient gas velocity within the porous portion of the distributor allows the gas to reach the decomposition temperature range. A variation of this gas distributor has been developed during the past four years at Oak Ridge National Laboratory.[4] To increase gas velocity, blind holes were drilled into the carbon to allow most of the gas to pass through the thinned regions. This design eliminated plugging but allowed particles

to stick to the porous carbon between the drilled holes. To minimize particle sticking to the frit, conical blind holes were drilled into the porous carbon as shown in Figs. 1(b) and 2. The high gas velocity through the thinned regions of this blind-hole frit keeps the entering gas below its decomposition temperature.

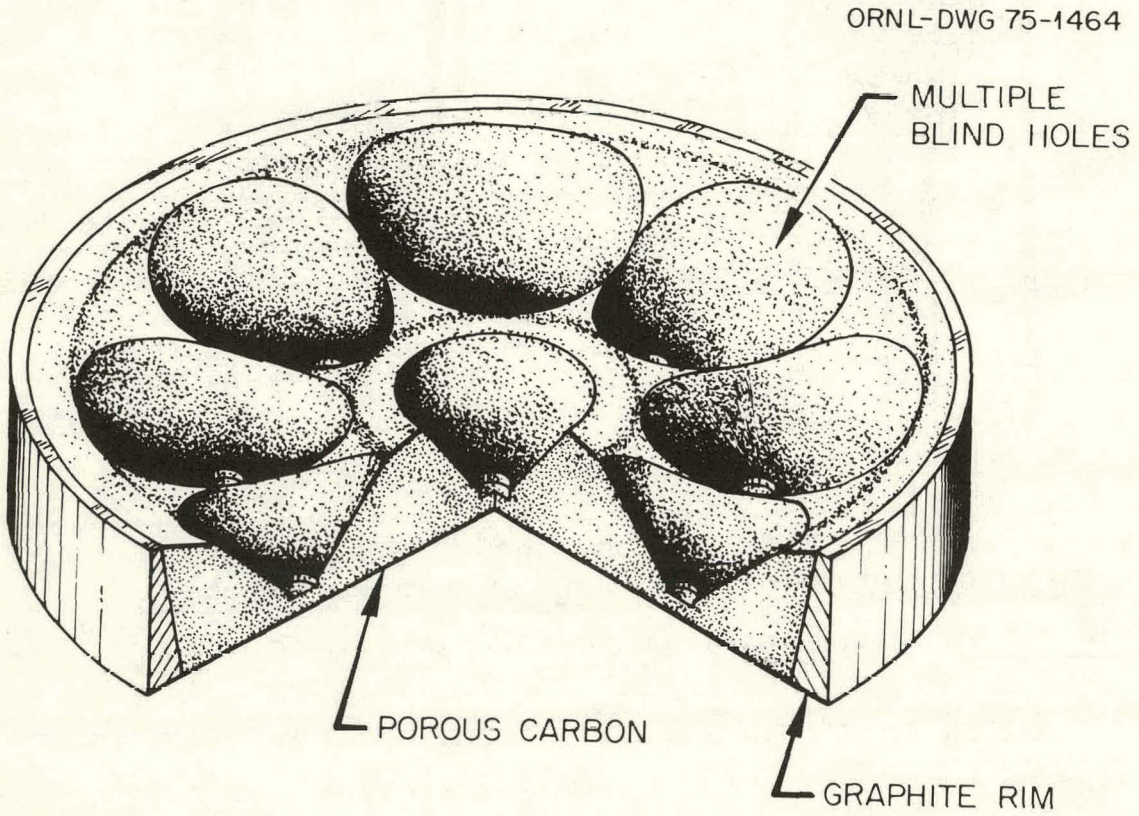

Fig. 2. Frit or Blind Hole Porous Plate Gas Distributor. The porous material is Grade 25 porous carbon available from Union Carbide Corporation.

An advantage of the new frit design is that the porous distributor and not the particle bed provides most of the resistance to gas flow. Therefore, localized variations in the quantity of particles above any particular gas inlet do not significantly alter the flow rate through that inlet.

One disadvantage of the frit is its higher fabrication cost compared with the simplest conical distributors. Both the cone and frit must be maintained after almost every coating run because of deposits on the

wall of the cone and the top of the frit. However, gas distributor costs are not large when compared with the total cost of fuel fabrication.[5] For small orders the cost of a single 24-cm-diam frit of the most complicated design tested to date is about $50, including the cost of materials as well as machining. Conservatively assuming that 3 kg of uranium can be processed per frit, we find then that the frit cost is only about 3% of the total cost involved in the fabrication of fresh fuel and about 1% of the cost for fabrication of recycle fuel. The costs for conical distributors may be about half that of the frit. However, the frit cost is not an overriding concern.

Another potential disadvantage of using the frit is the additional mechanical equipment necessary to unload a batch of particles. Equipment must be provided to lower the coating chamber from the furnace and unload the particles onto a scalping screen, which removes oversize debris that would otherwise interfere with pneumatic particle transfer. Figure 3 shows the coating furnace loop required when a frit is used in a remote facility, such as a hot cell, which is required for recycle fuel. Similar

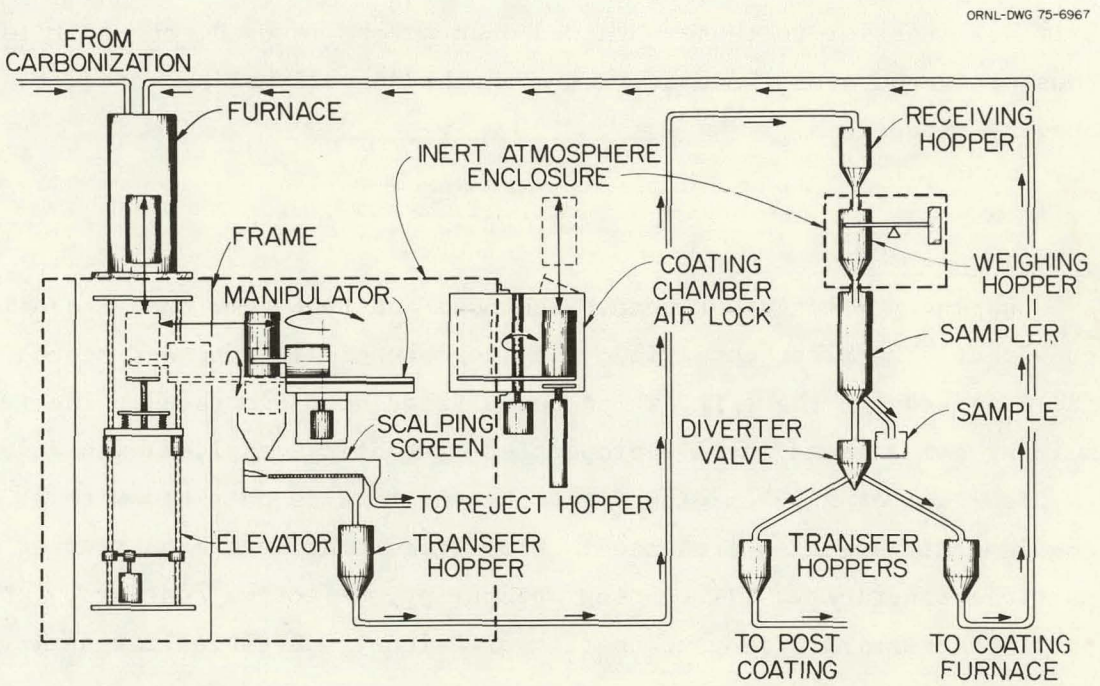

Fig. 3. Remote Coating Furnace Loop.

or perhaps the same equipment would probably be preferred for a fresh fuel plant. The majority of equipment (i.e., hoppers, sampler, weigher, scalping screen, and transfer lines) are required for either the cone or the frit. If a cone were used, one might expect that the inert-atmosphere enclosure would not be necessary because pyrophoric kernels could be drained through the hole in the cone directly into an inert-atmosphere container. However, the bottom of the furnace would likely be opened frequently for cone maintenance or replacement, and an inert-atmosphere enclosure around the furnace base might be desired to eliminate leakage of air into the open furnace. Also an inert-atmosphere enclosure might be necessary for off-normal situations where pyrophoric material fails to completely drain from the cone. The manipulator and elevator might also be needed for use with a conical distributor since some means is required for handling the cone and raising it into the furnace. Even with any added complexity of unloading particles when the frit is used, we believe that the frit system is mechanically more reliable and provides better material accountability than the system used with a cone. Since we will show that the coatings deposited with the frit are superior to those obtained when a cone is used, the frit is thus preferred over the cone from both the operational and product quality viewpoints.

RESULTS

During the last four years, the cone and frit have been extensively compared. The first comparison was the mechanical equipment needed for the cone and for the frit, which has already been discussed. The remaining comparisons involve properties of coatings applied with a 13-cm-diam cone or a 13-cm-diam frit. Recent results obtained with a 24-cm-diam frit are also presented. Properties that have been studied are particle sphericity, LTI coating anisotropy, defective coatings, whole-particle crushing strength, coating efficiency, particle loss during coating, standard deviation of coating thickness, and microstructure.

Particle Shape

Coated particles ideally should be nearly spherical to perform properly during irradiation. Particles become faceted during coating because carbon is deposited unevenly around the particle. An index termed "shape ratio" has been developed to measure the sphericity of coated particles.[6] The shape ratio is obtained for each particle by dividing the coating thickness on one side of a particle by the thickness on the opposite side. The particle shape for a batch is characterized by averaging 50 individual ratios. Figure 4 shows how the appearance of particles changes for shape ratios from 1.05 to 1.21.

A statistically designed experiment was conducted to determine how particle shape was influenced by the major process variables and by the type of gas distributor used. Forty-five coating runs were conducted with a 13-cm-diam coating furnace with a 30°-single-inlet conical gas distributor. Eight additional coating runs were made with various designs of the porous plate gas distributor. In each case the product was Biso-coated ThO_2. This experiment[6] showed that shape ratio was a function of coating rate and temperature, as seen in Fig. 5. The curves were fit by a multiple regression analysis of the 45 coating runs made with the cone. The shape ratios of coating runs made with the frit at 1375°C are also shown on this graph, and these data points should be compared with the curve labeled 1375°C. The frit produced coatings with shape ratios lower than any of the similar runs using the conical gas distributor. The shape ratio ranged from 1.06 to 1.09 for the porous plate runs compared with 1.13 to 1.16 for the similar conical runs. The 95% confidence intervals for the mean shape ratio for particles coated by use of the porous plate and the cone do not overlap. Similar results were obtained for Triso-coated fissile particles.[7]

LTI Anisotropy

During irradiation graphitic materials undergo considerable anisotropic dimensional changes. They expand in the c direction and contract

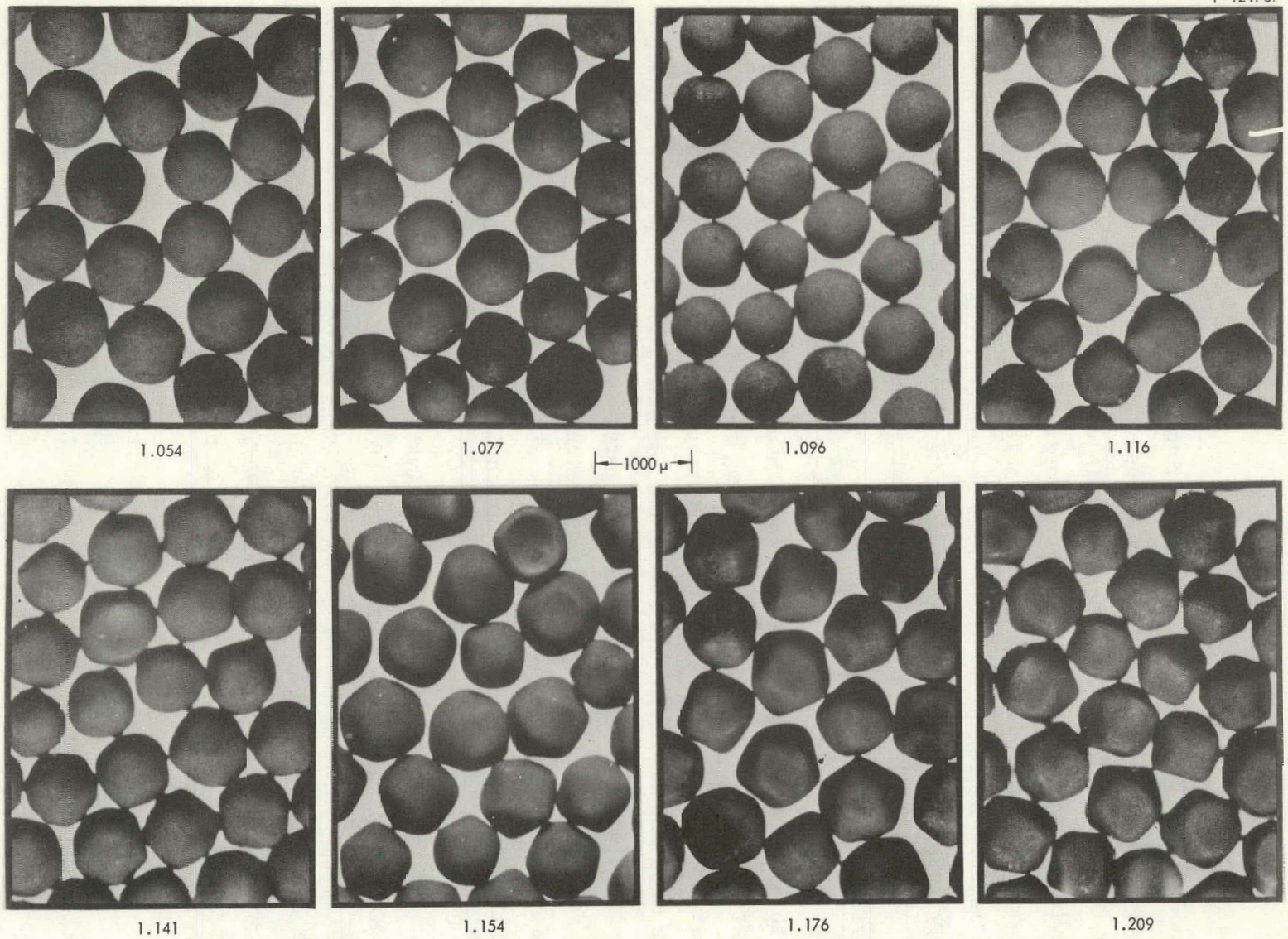

Fig. 4. Comparison of LTI Shape Ratio with Macrographs of Biso-Coated Particles.

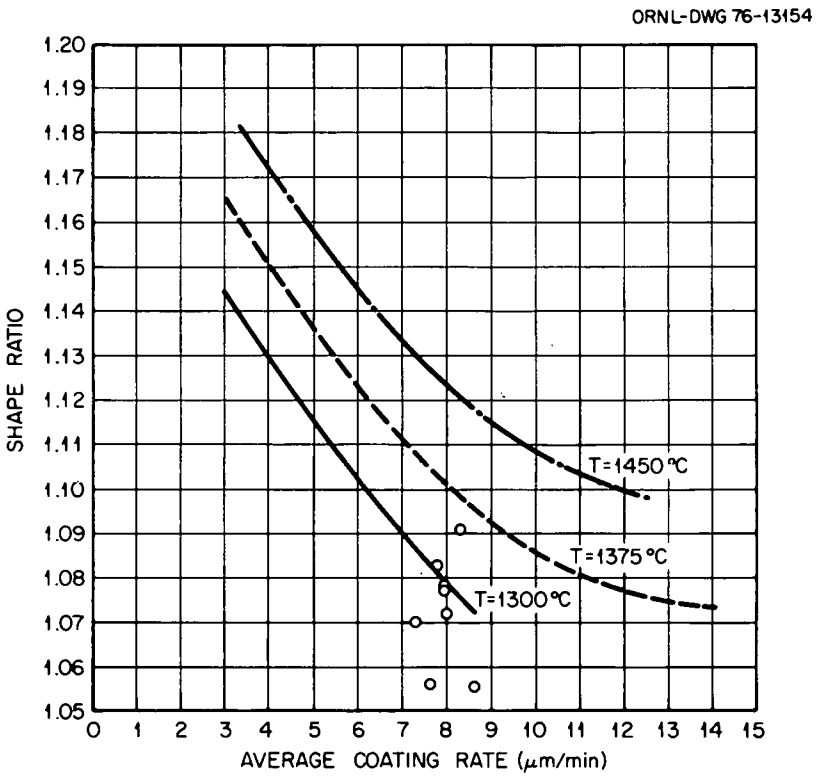

Fig. 5. Influence of Coating Rate, Temperature, and Gas Distributor Type on LTI Faceting. The curves are from a multiple regression analysis of 45 coating runs made with a conical gas distributor. The data points are for runs made at 1375°C with several blind-hole frit designs.

in the orthoganal directions. The LTI layers of coated fuel particles must be quite isotropic to avoid the generation of high stresses during irradiation.

Particles from the experiment on LTI faceting described above were also used to examine the effect that coating variables and gas distributor type have on the anisotropy of LTI coatings. The Bacon anisotropy factor as determined optically (BAF_o) was measured by General Atomic Company for all the coatings. The BAF_o depended on the coating rate, in agreement with other investigations.[8] Anisotropy values for coatings applied with the cone and frit are shown in Fig. 6. The BAF_o values of all the coatings applied with the frit are lower than any values for coatings applied with the cone. The anisotropy difference is more striking if one compares coatings deposited at the same deposition

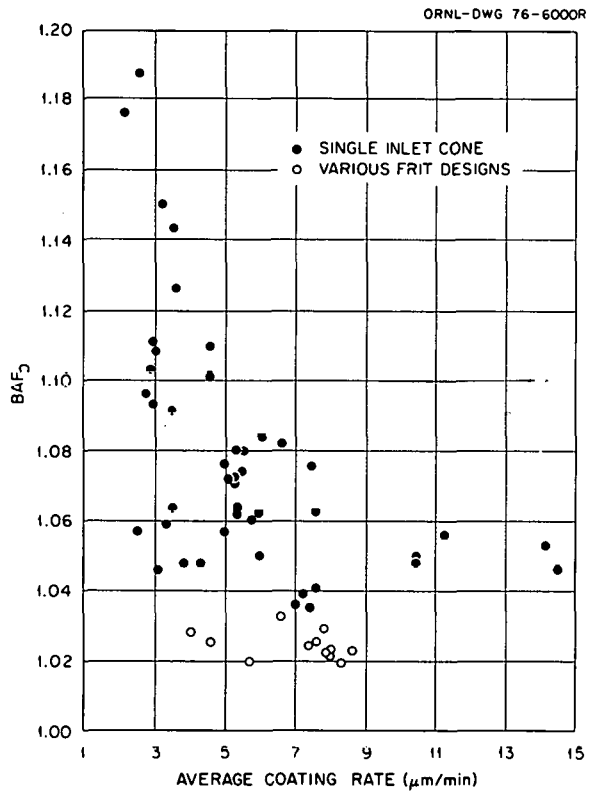

Fig. 6. Influence of Coating Rate on BAF_o for LTI Coatings Deposited with a 13-cm-diam Cone or Frit.

temperature and rate. The curves of Fig. 7 were found by a multiple regression analysis for the 45 coating runs made with the cone. The lines of Fig. 7 show that a large amount of the scatter in the data of Fig. 6 for the cone runs is accounted for by the effect of deposition temperature. The deposition temperature effect was shown to be statistically significant at the 99% confidence level. The points in Fig. 7 are for coatings deposited at 1375°C by use of the frit. Comparison of these points with the line labeled 1375°C in Fig. 7 shows that the frit produces coatings having BAF_o values about 0.02 to 0.04 units lower than coatings similarly deposited with a cone. This is potentially a significant effect when viewed in terms of the ability of the coatings to survive irradiation to high neutron fluences. The reason for the lower BAF_o values obtained with the frit is unknown but may be related to the more uniform distribution of coating gas.

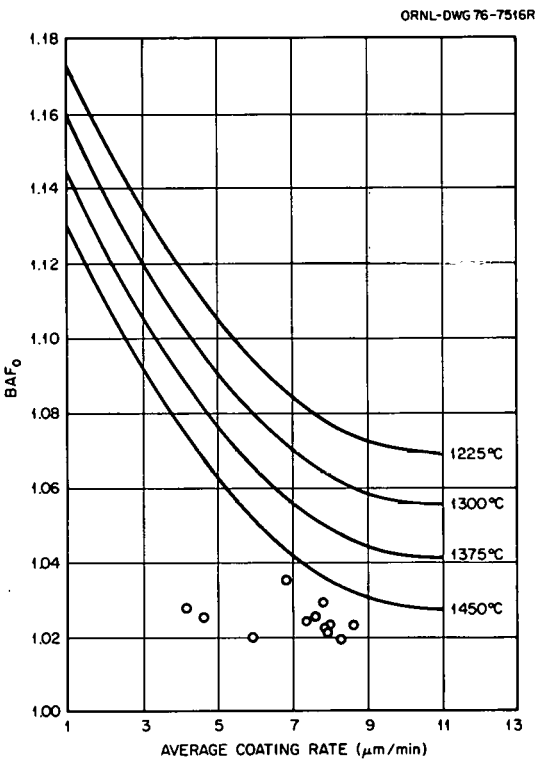

Fig. 7. Correlation of BAF_o with Coating Rate, Temperature, and Gas Distributor. The curves are from a multiple regression analysis of 45 coating runs made with a conical gas distributor. The data points are for runs made at 1375°C with several blind-hole frit designs. The curves and points are for a propylene flow rate of 0.17 std liter/sec. (3.6 scfm).

Perhaps a more important factor than the average BAF_o value for a particle batch is the fraction of the particles that have a BAF_o value greater than some critical value above which an appreciable fraction of coatings would fail during irradiation. Thus the particle-to-particle variation in BAF_o within the batch as measured by the standard deviation is important. Particles coated in a 13-cm-diam cone under typical coating conditions had a standard deviation of 0.011, while particles coated with a 13- or 24-cm-diam frit had a standard deviation of about 0.004. The lower standard deviation for particles coated with the frit implies greater uniformity of the coating conditions from place to place within the fluidized bed. Also, two factors contribute to lower standard deviations for particles coated with the frit. For a given batch of particles, typically the BAF_o values for individual particles show a negative correlation with coating thickness (i.e., low BAF_o values are observed for

particles having thick coatings). Similarly, for a given particle the BAF_o varies from point to point around the particle depending on the localized value of coating thickness (i.e., thick portions of the coating tend to have low BAF_o values and thin portions high values). The effects of both the particle-to-particle variation in thickness and the within-particle thickness variation contribute to lower standard deviations for particles coated with the frit since these variations in thickness are less pronounced.

For both the cone and frit, the within-batch standard deviation of BAF_o is correlated with the average BAF_o for the batch; standard deviation decreases with decreasing values of mean BAF_o, as shown in Fig. 8. Note that coatings deposited with the 24-cm-diam frit have low values for both the mean BAF_o and the standard deviation of BAF_o.

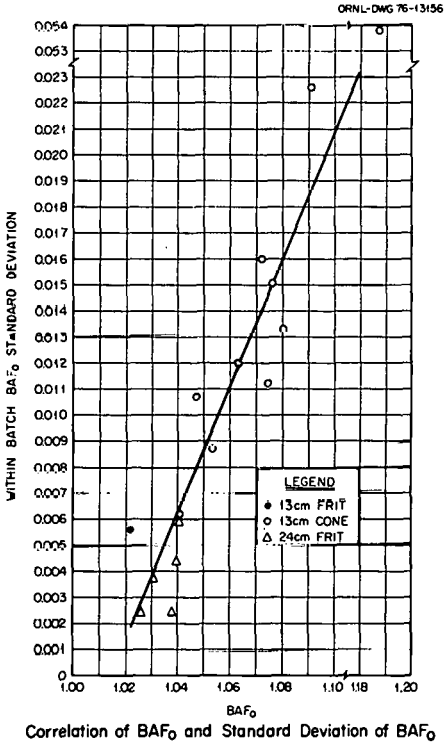

Fig. 8. Correlation of BAF_o and Standard Deviation of BAF_o. Note the breaks in the scales.

The importance of the particle-to-particle variation in BAF_o is shown in Fig. 9. Here the within-batch distribution of BAF_o values is given for typical frit and cone batches. For the frit batch, note that only 0.6 and 0.01% of the particles have BAF_o values that exceed 1.04 and 1.045, respectively. In comparison, about 3% of the particles coated

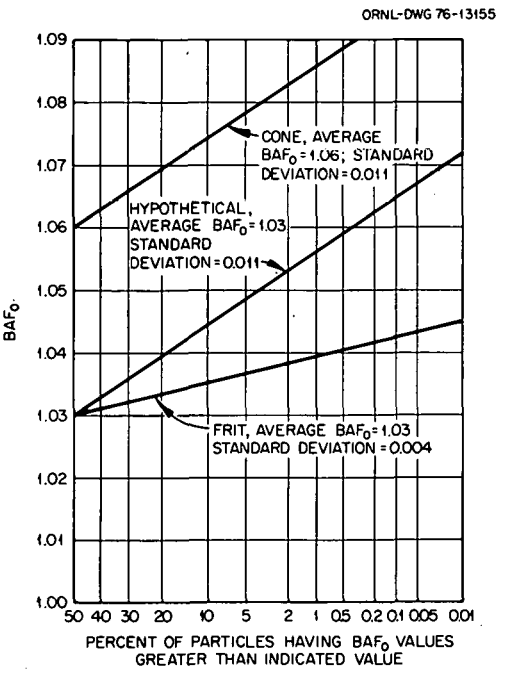

Fig. 9. Particle-to-Particle Variation in LTI Anisotropy.

with a cone have BAF_o values exceeding 1.08. The line in Fig. 9 labeled "hypothetical" shows the importance of standard deviation. For this line, the average BAF_o value is low (1.03), but because of the high standard deviation (0.011) the fraction of particles having high BAF_o values is much larger than for the particles coated with the frit.

Excessive variation of BAF_o through the coating within a given particle could generate stress within the LTI coating as dimensions change during irradiation. The data of Fig. 10 show that such variation need not be excessive. The figure shows the radial variation in BAF_o across the LTI coating for three randomly chosen Biso-coated ThO_2 particles. The coatings had been deposited with a 24-cm-diam frit and a constant flow of diluted propylene. Two opposing effects were likely

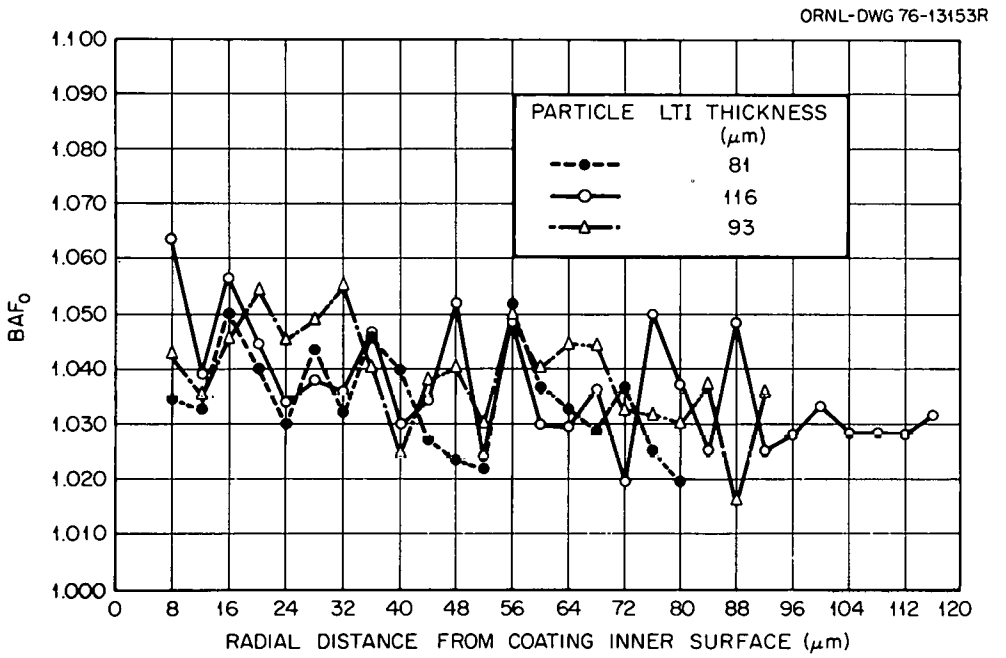

Fig. 10 Within-Particle Variation in LTI Anisotropy.

present: (1) a tendency for the BAF_o to increase with increasing thickness because of a decrease in the deposition rate as the surface area of the particles increased and (2) a tendency for the BAF_o to decrease with increasing radial distance since the coating furnace temperature during all but the initial portion of the run was increasing with time. Initially the temperature suddenly dropped because of the cooling effect of propylene decomposition then gradually increased to the set point as a result of a higher power input to the furnace heater. Apparently the two effects nearly cancelled since the net result was only a slight decrease in BAF_o with location.

Defective Coatings

The fraction of particles that are defective is determined[9] by leaching with gaseous chlorine at 1500°C for 2 hr. A Biso-coated particle is said to be defective if the LTI layer is either cracked or permeable. In a previous study[10] with Biso-coated ThO_2, the fraction defective, as shown in Fig. 11, depended on LTI thickness, coating gas dilution, and whether the particles were annealed or not. Each line is a

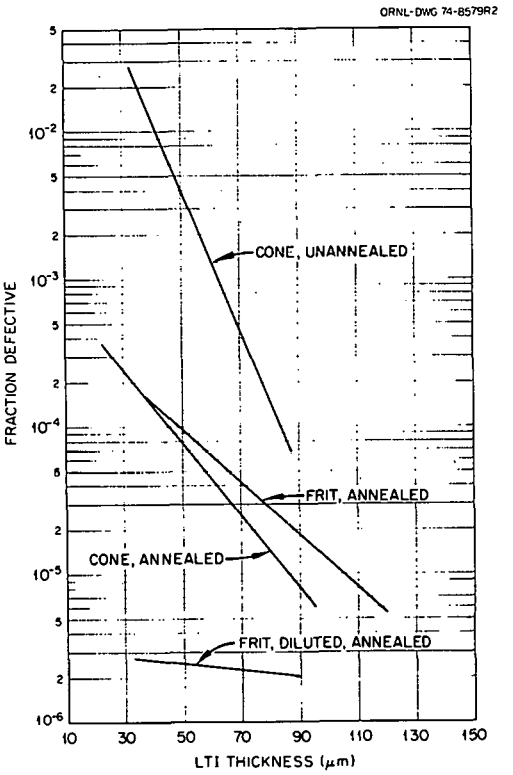

Fig. 11. Effect of Coating Thickness and In-Place Annealing on As-Coated Defective Particle Fraction for Biso-Coated ThO_2.

least squares fit of 10 to 50 different coating runs. Unannealed coatings applied with the cone onto buffer-coated thoria yield high defective fractions because stresses generated during coating deposition cause many coatings to crack when subjected to additional stresses during cooling.[10] Cracked coatings are eliminated by annealing before cooling from the coating temperature, and thus for the two lines in the center of Fig. 11, permeable coatings account for the observed defective particles; the slightly higher defective fraction for the frit is the result of either scatter in the data or the use of higher deposition rates for the particles coated with the frit.

Recently unannealed LTI coatings were applied with the 13- and 24-cm-diam frits. The results indicate that these coatings do not crack on cooling, contrary to results obtained with the 13-cm-diam cone. This

indicates that the frit produces coatings with lower stresses than the cone, perhaps because more uniform deposition conditions yield less radial variation in the properties of the coating.

The fraction of SiC coatings that are cracked is of great importance as regards fission product release from fissile fuel particles. An extensive amount of data shows that the SiC defective fraction is less than the target value of 1×10^{-4} for coatings deposited with a 13-cm-diam frit. Limited comparisons indicate that the defective fraction is less than that obtainable with a cone. The defective fraction for the one SiC run made with a 24-cm-diam frit was 3×10^{-5}.

Particle Crushing Strength

Whole-particle crushing strength has been studied for Biso and Triso coatings deposited with either the cone or the frit.[11] Typically, gas distributor type does not significantly influence crushing strength of Biso-coated particles. Triso-coated particles annealed at the conditions used for fuel rod annealing (i.e., 1800°C for 30 min) have higher crushing strengths when coated with the frit rather than the cone.[11]

Efficiency

Coating efficiency (i.e., the percent of the input carbon that ends up as coating on the particles) is of interest. Low efficiency complicates furnace effluent handling, wastes coating gas, and increases the run time. Coating efficiency depends on coating conditions but is consistently higher for the frit than the cone. The higher efficiency is likely the result of improved gas-solid contact. During buffer coating the efficiency is typically 60% for the frit and about 50% for the cone. The efficiency is also higher with the frit for the LTI coating process, as shown in Fig. 12. In this comparison, the coating conditions were constant and only the duration of the run was varied.

Very high coating efficiencies were obtained with the 24-cm-diam frit. Typically, the buffer and LTI coating efficiencies were 70 and 50–65%, respectively.

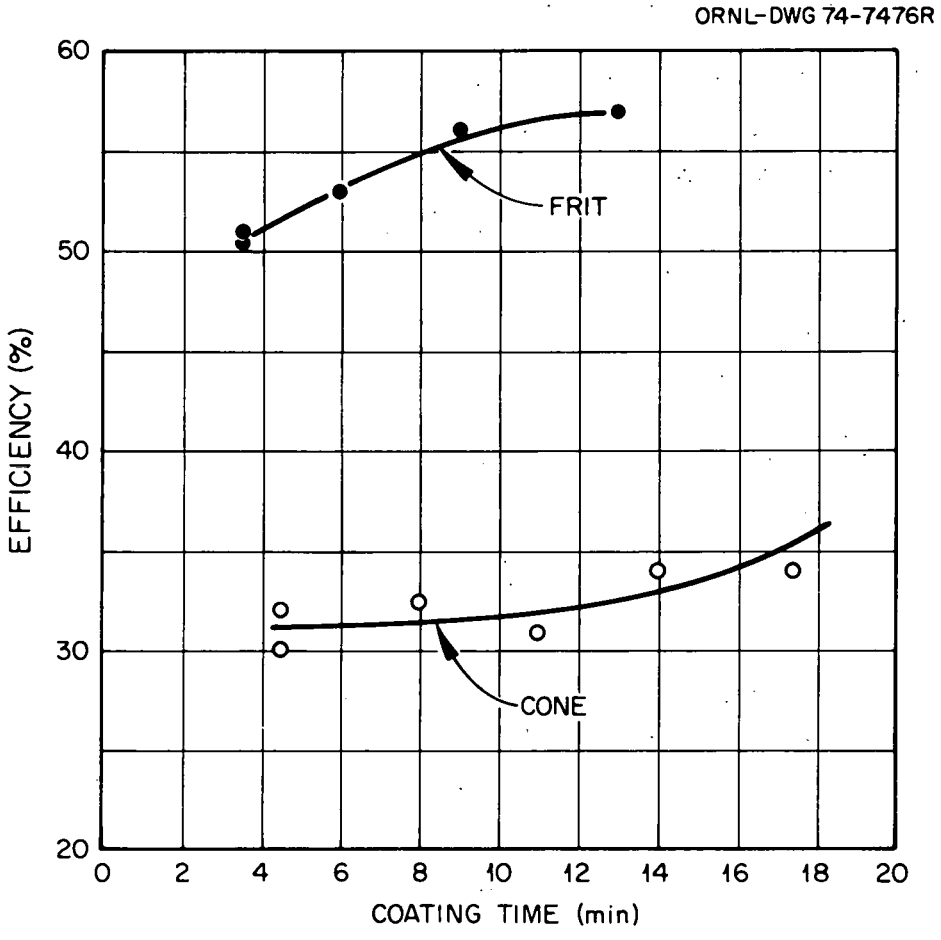

Fig. 12. Comparison of Cone and Frit Coating Efficiency for the LTI Coating Process in a 13-cm-diam Furnace.

Kernels Recovered

The number of particles "lost" during coating by carry-over into the gas exhaust system or sticking to furnace components must be kept to a minimum. The loss depends on furnace height, gas flow rate, quantity of particles being coated, etc. Accurate measurements are difficult to make, but a large amount of data indicates the loss for the cone and frit in our 13-cm-diam furnace to be less than 1%. There is an indication that the total loss is less for the frit. This is to be expected since, although more particles adhere to the frit than to the cone, the uniform dispersion of gas obtained with the frit results in less violent eruptions of the particle bed. Observations of hot fluidized beds show less throwing of particles with the frit.

Coating Thickness Standard Deviation

Within-batch particle-to-particle variation in coating thickness is important since particles having a coating layer thinner than some critical value are more likely to fail during irradiation. For the buffer coating process, the coating thickness variation is practically the same for the cone and frit. For the LTI coating process less variation in coating thickness is observed for particles coated with the frit. Thickness standard deviation values depend on a number of process and particle design variables, but typical values for the relative standard deviation for LTI thickness for particles coated in a 13-cm-diam furnace are 9% for the cone and 7% for the frit.

Microstructure

The LTI coatings deposited with a frit have a more uniform microstructural appearance than coatings deposited with a cone, as is evident in Figs. 13 and 14. When a polished surface is viewed with bright-field illumination at 100 to 500× frit-deposited coatings show noticeably less tendency for pores or soot inclusions to preferentially align to yield an onion-peel structure. This should result in less tendency for coatings deposited with the frit to delaminate and fail as a result of irradiation-induced dimensional changes. The more uniform structure obtained with the frit is likely the result of more uniform deposition conditions.

Scale-Up to Commercial Furnace Size

Coating furnaces for commercial operations are expected to be about 24-cm in diameter. Although a large amount of data showed the frit type of gas distributor to be preferable for 13-cm-diam furnaces, it was not known whether the frit could be successfully scaled to 24-cm-diam. The porous carbon portion of the gas distributor is not strong and thus large frits might not withstand the load of particles above them or the force exerted by the coating gas supply below them. To answer the scale-up question, four frit designs were recently tested in a 24-cm-diam

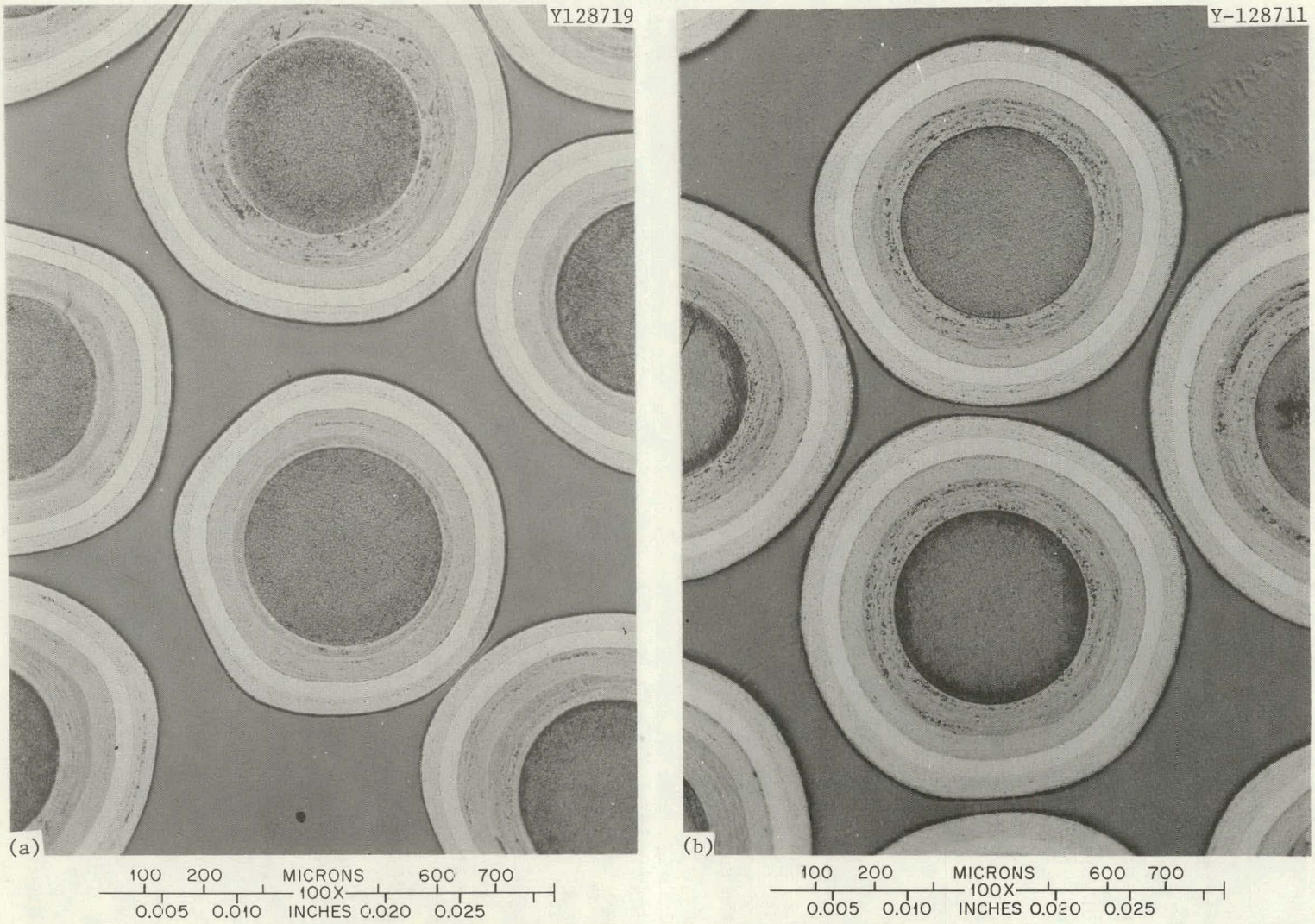

Fig. 13. Comparison of the Microstructure of Coatings Deposited with (a) Cone and (b) Frit. In both cases the particles are of the Triso-coated fissile type.

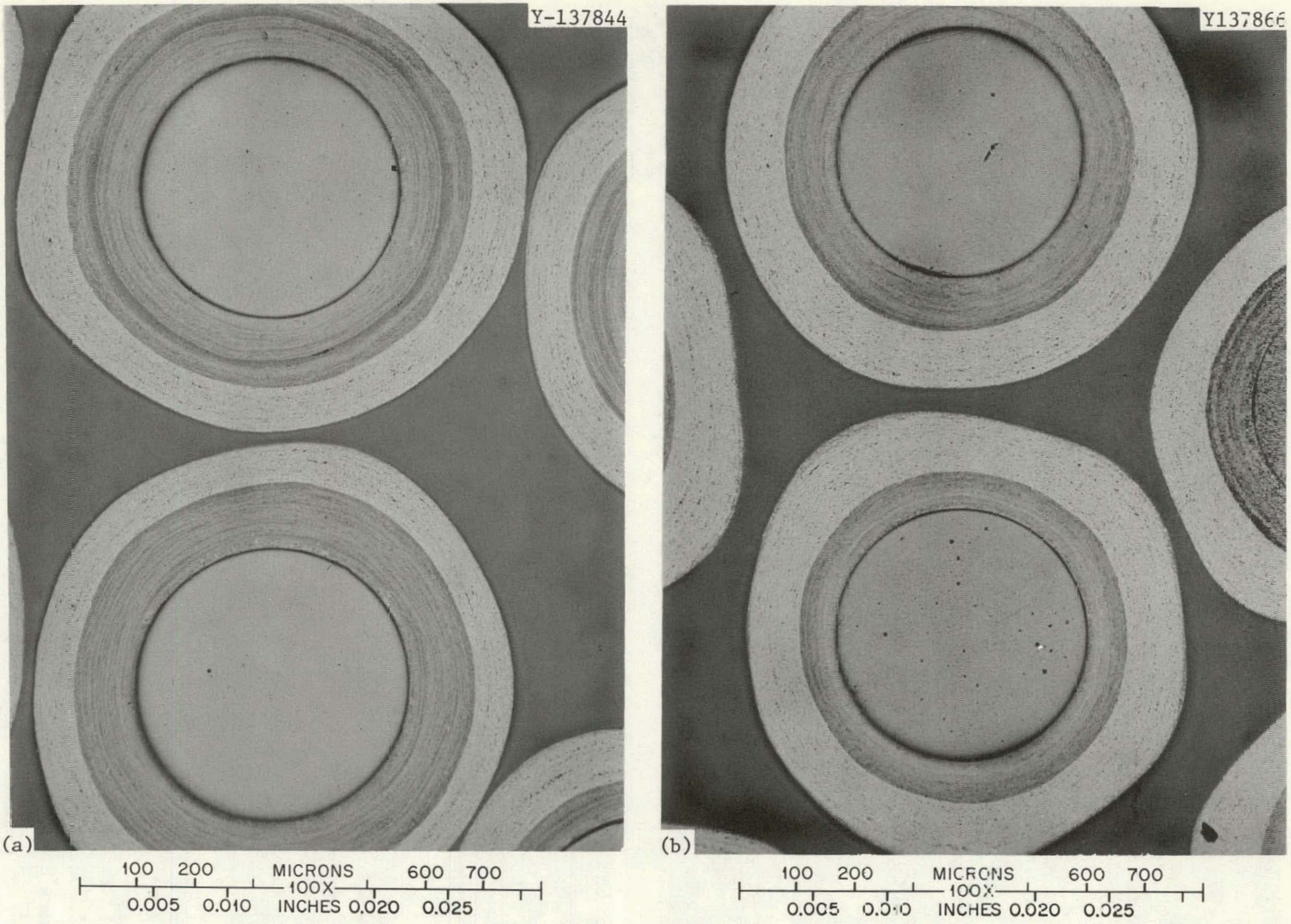

Fig. 14. Biso-Coated ThO_2 Prepared with the 24-cm-diam Frit having 25 Holes. (a) LTI deposited from C_3H_6. (b) LTI deposited from mixture of C_2H_2 and C_3H_6. The striations in the buffer layer should be ignored because of excessive cycling of the acetylene flow rate.

coating furnace. These were:

1. 24-cm-diam frit, 25 blind holes, as shown in Fig. 15;
2. 24-cm-diam frit, 13 blind holes;
3. 24-cm-diam frit, 9 blind holes; and
4. 13-cm-diam frit, 9 blind holes, located at the lower end of a cone, which flared to 24-cm in diameter.

Eight Biso coating runs and one SiC run were conducted. Designs 1 through 3 each performed very satisfactorily, with perhaps design 1 being slightly preferable. Type 4 was unsatisfactory; particle bed movement was more typical of that of a cone in that it tended toward slugging rather than uniform fluidization, and carbon coating efficiencies and coating properties were inferior to those obtained with the other three designs. All characterization data for the best Biso-coated particle batch indicate that the particles should have good irradiation performance. For this batch, the BAF_o averaged 1.033, and the defective fraction was 2×10^{-5}, as determined by the chlorine leach test. The defective fraction for the SiC-coated particles was 3×10^{-5}, and the SiC density was 3.206 g/cm^3; both values being very acceptable. All indications were that scale-up was feasible.

CONCLUSIONS

A comparison of equipment, process responses, and product quality showed that a new multiple-inlet porous-plate gas distributor is preferred over conical gas distributors for coating of HTGR fuel particles. Principal advantages of the porous plate distributor are simplicity, high assurance that particles will not drain from the coater during upset conditions, improved material accountablilty, and more uniform gas distribution, which leads to superior coating properties. Properties that are improved are particle sphericity, LTI isotropy, LTI thickness standard deviation, LTI microstructure, and LTI and SiC defective fraction. The new distributor appears ideally suited for scale-up to commercial-size coating furnaces.

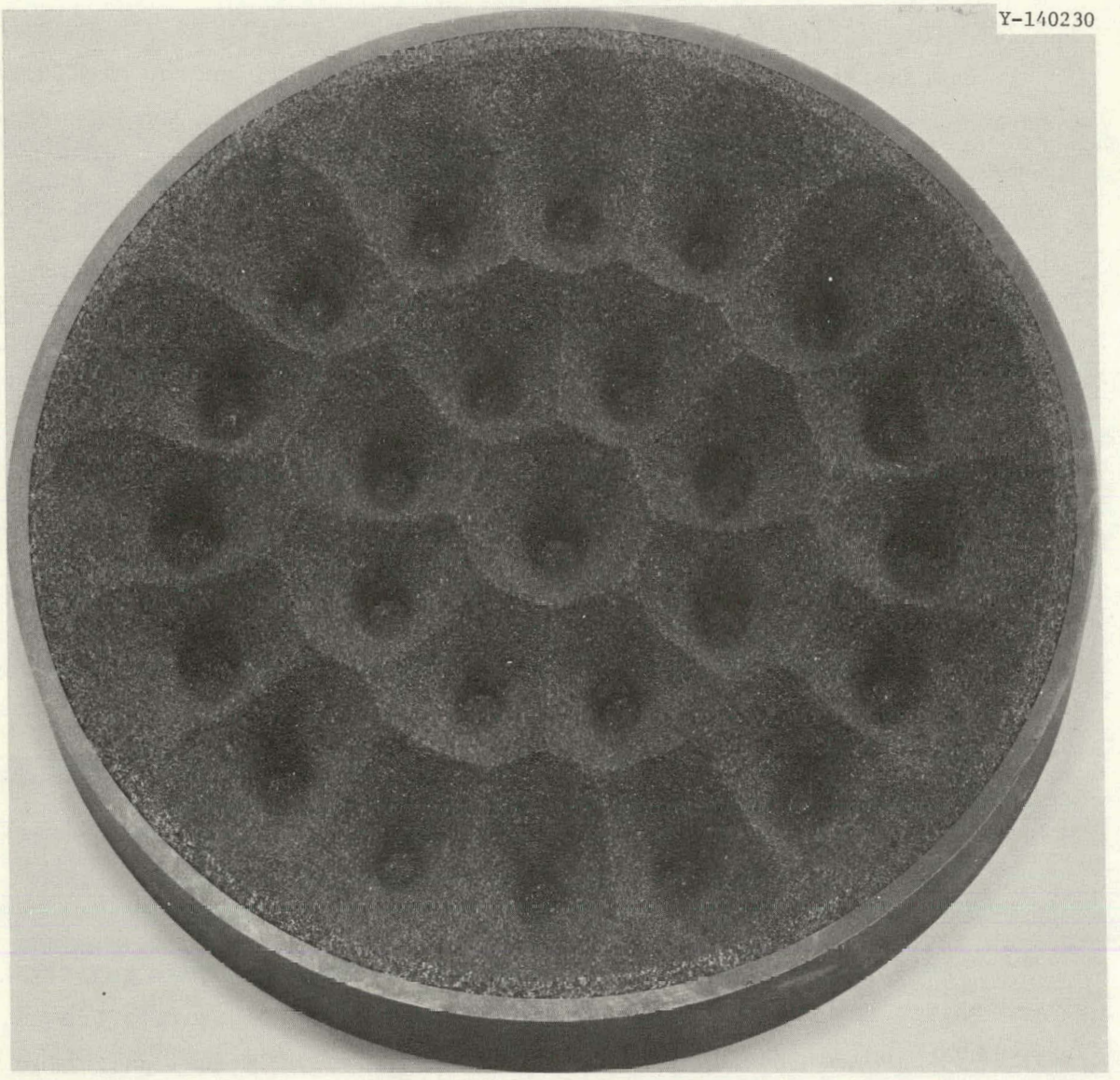

Fig. 15. Porous-Plate Gas Distributor, 24-cm-diam with 25 Blind Holes.

ACKNOWLEDGMENTS

The assistance of M. K. Preston, R. R. Suchomel, and D. Kiplinger in the design, fabrication and cold checkout of equipment used in the 24-cm-diam coating furnace is greatly appreciated. Numerous members of the staff of General Atomic Company are thanked for their assistance in testing the 24-cm-diam frits. We are grateful to C. E. DeVore and J. B. Flynn for their careful work during the coating of particles and measurement of coating thickness.

The manuscript was edited by Sigfred Peterson and prepared for submission for publication by Gail Golliher of the Metals and Ceramics Division Reports Office.

REFERENCES

1. R. B. Pratt, J. D. Sease, W. J. Pechin, and A. L. Lotts, "Pyrolytic Carbon Coating in an Engineering-Scale System," *Nucl. Appl.* 6(3): 241–55 (March 1969).
2. W. J. Lackey et al., "Microsphere Coating," *Gas-Cooled Reactor and Thorium Utilization Program Annu. Progr. Rep. Sept. 30, 1971,* ORNL-4760, pp. 45–52.
3. R. L. Pilloton, *Fluidized-Bed Coating Apparatus,* (to U.S. Atomic Energy Commission). U.S. Patent 3,889,631. August 27, 1968.
4. W. J. Lackey and J. D. Sease, *Means for Effecting Fluidization in Pyrolytic Carbon Coating Processes* (to U.S. Atomic Energy Commission). U.S. Patent 3,889,631. June 17, 1975.
5. P. R. Kasten et al., *Assessment of the Thorium Fuel Cycle in Power Reactors,* ORNL/TM- 5565 (in press).
6. W. J. Lackey, W. H. Pechin, and J. D. Sease, "Measurement and Control of Shape of Fuel Particles for High-Temperature Gas-Cooled Reactors," *Am. Ceram. Soc. Bull.* 54(8): 718–24 (August 1975).
7. D. P. Stinton, W. J. Lackey, and D. R. Johnson, "Process Development," *Gas-Cooled Reactor Programs Thorium Utilization Program Prog. Rep. Jan. 1, 1974 through June 30, 1975,* ORNL-5128, pp. 158–65.

8. D. W. Stevens, "Optical Anisotropy in Nearly Isotropic Pyrolytic Carbons," pp. 167–68, *Eleventh Biennial Conference on Carbon*, Gatlinburg, Tennessee (1973), Paper SS-3, CONF-730601.

9. D. E. LaValle, D. A. Costanzo, W. J. Lackey, and A. J. Caputo, *The Determination of the Defective Particle Fraction in HTGR Fuels*, ORNL/TM-5483 (in press).

10. W. J. Lackey, J. D. Sease, D. A. Costanzo, and D. E. LaValle,"Improved Coating Process for High-Temperature Gas-Cooled Reactor Fuel," *Trans. Am. Nucl. Soc.* 22: 194–95 (November 1975).

11. W. J. Lackey, D. P. Stinton, L. E. Davis, and R. L. Beatty, "Crushing Strength of HTGR Fuel Particles," *Nucl. Technol.* 31(2): 191–201 (November 1976); ORNL/TM-5132

ORNL/TM-5731

Category
Distribution UC-77

INTERNAL DISTRIBUTION

1–2. Central Research Library
3. Document Reference Section
4–11. Laboratory Records Department
12. Laboratory Records, ORNL RC
13. ORNL Patent Office
14. P. Angelini
15. B. J. Baxter
16. R. A. Bradley
17. C. R. Brinkman
18. A. J. Caputo
19. J. A. Carpenter
20. J. H. Coobs
21. D. Costanzo
22. J. E. Cunningham
23. F. C. Davis
24. J. H. DeVan
25. J. R. DiStefano
26. R. G. Donnelly
27. W. P. Eatherly
28. J. I. Federer
29. P. A. Haas
30. C. C. Haws
31. R. L. Hamner
32–34. M. R. Hill
35. F. J. Homan
36. J. D. Jenkins
37. D. R. Johnson
38. M. J. Kania
39–40. P. R. Kasten
41. R. K. Kibbe
42–46. W. J. Lackey
47. D. E. LaValle
48. B. C. Leslie
49. T. B. Lindemer
50. A. L. Lotts
51. J. E. Mack
52. W. R. Martin
53. R. W. McClung
54. H. E. McCoy
55. D. L. McElroy
56. C. J. McHargue
57. S. R. McNeany
58. C. S. Morgan
59. M. T. Morgan
60. K. J. Notz
61. A. P. Olsen
62. A. E. Pasto
63. P. Patriarca
64. R. L. Pearson
65. W. H. Pechin
66. H. Postma
67. J M Robbins
68. J. E. Rushton
69. T. F. Scanlan
70. A. C. Schaffhauser
71. J. L. Scott
72. J. D. Sease
73. J. H. Shaffer
74. J. W. Snider
75. J. O. Stiegler
76–78. D. P. Stinton
79. R. R. Suchomel
80. V. J. Tennery
81. S. M. Tiegs
82. T. N. Tiegs
83. D. B. Trauger
84. J. E. Van Cleve
85. G. C. Wei
86. J. R. Weir, Jr.
87. R. G. Wymer
88. R. M. Young
89. C. S. Yust
90. P. M. Brister (consultant)
91. J. Moteff (consultant)
92. H. Palmour III (consultant)
93. J. W. Prados (consultant)
94. N. E. Promisel (consultant)
95. D. F. Stein (consultant)

EXTERNAL DISTRIBUTION

96–103. ERDA DIVISION OF NUCLEAR FUEL CYCLE AND PRODUCTION, Washington, D.C. 20545

Director
R. G. Bradley
W. S. Schieb

104–105. ERDA DIVISION OF REACTOR NUCLEAR RESEARCH AND APPLICATIONS, Washington, D.C. 20545

Director

106–107. ERDA IDAHO OPERATIONS OFFICE, P.O. Box 2108, Idaho Falls, ID 83401

C. E. Williams, Manager
Barry Smith

108. ERDA OFFICE OF PROGRAM MANAGEMENT, RESEARCH AND SPACE PROGRAMS, P.O. Box 81325, San Diego, CA 92138

J. B. Radcliffe

109. ERDA SAN FRANCISCO OPERATIONS OFFICE, 1333 Broadway, Wells Fargo Bldg., Oakland, CA 94612

R. D. Thorne, Manager

110–112. ERDA OAK RIDGE OPERATIONS OFFICE, P.O. Box E, Oak Ridge, TN 37830

Director, Research and Technical Support Division
Director, Reactor Division
F. E. Dearing, Reactor Division

113–176. ERDA TECHNICAL INFORMATION CENTER, P.O. Box 62, Oak Ridge, TN 37830

For distribution as shown in TID-4500 Distribution Category, UC-77 — Gas-Cooled Reactor Technology

☆ U.S. GOVERNMENT PRINTING OFFICE: 1977-748-189/143